

# Opt4GPTQ: Co-Optimizing Memory and Computation for 4-bit GPTQ Quantized LLM Inference on Heterogeneous Platforms

1<sup>st</sup> Yaozheng Zhang

*School of Computer Science and Engineering  
Shandong University of Science and Technology  
Qingdao, China  
yaozheng.zhang@sdust.edu.cn*

2<sup>nd</sup> Wei Wang

*School of Computer Science and Engineering  
Shandong University of Science and Technology  
Qingdao, China  
wei\_wang@sdust.edu.cn (Corresponding author)*

3<sup>rd</sup> Jie Kong

*School of Computer Science and Engineering  
Shandong University of Science and Technology  
Qingdao, China  
jiekong0112@sdust.edu.cn*

4<sup>th</sup> Jiehan Zhou

*School of Computer Science and Engineering  
Shandong University of Science and Technology  
Qingdao, China  
jiehan.zhou@sdust.edu.cn (Corresponding author)*

5<sup>th</sup> Huanqing Cui

*School of Computer Science and Engineering  
Shandong University of Science and Technology  
Qingdao, China  
cuihq@sdust.edu.cn*

**Abstract**—The increasing adoption of large language model (LLMs) on heterogeneous computing platforms poses significant challenges for achieving high inference efficiency. To address the low inference efficiency of LLMs across diverse heterogeneous platforms, this paper proposes a practical optimization method, Opt4GPTQ, designed for 4-bit GPTQ quantized LLMs inference on heterogeneous AI accelerators. Built upon the vLLM serving system, Opt4GPTQ integrates three platform-level optimization strategies: Shared Memory Buffering optimization (SMB-Opt), which caches data in shared memory and employs single-threaded writes; Vectorized Memory Loading optimization (VML-Opt), which utilizes vectorized memory operations for efficient data loading; and Inline Assembly optimization (ILA-Opt), which directly leverages hardware-native vector half-precision addition and fused multiply-accumulate instructions for efficient execution. Experimental results show that Opt4GPTQ effectively improves inference performance across different models, achieving up to 84.42% throughput improvement and up to 51.35% latency reduction. This work highlights the critical role of platform-level engineering optimizations in enabling efficient LLMs inference on emerging heterogeneous AI acceleration architectures and provides valuable deployment experience and methodologies for future heterogeneous platform adaptation.

**Index Terms**—vLLM, Inference Efficiency, Platform-level Optimization, GPTQ 4-bit Quantization, Heterogeneous Computing Platforms.

## I. INTRODUCTION

Large Language Models (LLMs), such as Llama [1], ChatGPT [2], DeepSeek-V2 [3], and Gemini [4], have demonstrated broad application potential in tasks like conversational agents and text generation. However, their substantial

parameter scales, coupled with high computational loads, memory access overhead, and memory consumption during inference, present significant challenges for achieving efficient execution. These issues are particularly pronounced in resource-constrained edge environments and remain critical in cloud scenarios where performance and energy efficiency are paramount. Consequently, enhancing inference efficiency while maintaining model accuracy has become a key focus of current research [5], [6].

To address these challenges, the virtual Large Language Model (vLLM) serving system was proposed [7]. vLLM optimizes key-value (KV) cache management by flexibly sharing KV caches across single and multiple requests, thereby reducing overall memory usage. In addition, vLLM supports various low-bit quantization techniques, leveraging low-precision weights and activations combined with optimized compute cores (e.g., INT8/INT4 Tensor Cores) to accelerate inference [8], [9]. Among weight-only quantization methods, Generative Pre-trained Transformer Quantization (GPTQ) has attracted attention for its ability to achieve 4-bit quantization while maintaining acceptable inference accuracy [10]. GPTQ combines one-shot weight quantization with approximate second-order information, enabling large-scale LLMs to be compressed to 4-bit precision in a relatively short time with minimal accuracy degradation, making it one of the mainstream low-bit quantization approaches.

Although vLLM and GPTQ have achieved mature performance optimizations on conventional accelerator platforms

such as GPUs, the emergence of heterogeneous computing platforms introduces new hardware architectures that pose additional adaptation challenges. By integrating CPUs with GPUs, NPUs, or other domain-specific accelerators, heterogeneous platforms offer new opportunities to enhance Large Language Model (LLM) inference efficiency [11], [12]. However, significant architectural differences among platforms hinder the direct deployment of GPU-optimized inference frameworks on these accelerators, making hardware-specific adaptation and performance tuning critical issues to address.

The Deep Computing Unit (DCU) is a heterogeneous accelerator designed for AI workloads [13]. It adopts a general-purpose GPGPU architecture and maintains full compatibility with the ROCm ecosystem, theoretically ensuring CUDA compatibility. However, due to insufficient exploitation of the underlying hardware architecture by current inference engines, the inference performance on DCU has not yet reached its expected potential. In particular, in quantized inference scenarios, issues such as throughput degradation and increased latency significantly limit the performance scalability of LLM inference on DCU.

To tackle these challenges, this paper presents a systematic engineering optimization and adaptation study of the 4-bit GPTQ quantized inference kernel in the vLLM serving system on the DCU heterogeneous accelerator platform, proposing the Opt4GPTQ approach. This approach integrates three optimization strategies: Shared Memory Buffering Optimization (SMB-Opt), which caches data in shared memory and employs single-threaded writes to reduce global memory access overhead; Vectorized Memory Loading Optimization (VML-Opt), which utilizes vectorized memory operations for efficient data loading; and Inline Assembly Optimization (ILA-Opt), which directly utilizes the hardware’s native vectorized half-precision addition and fused multiply-add instructions for efficient execution. The proposed optimization methods and engineering practices provide valuable references for LLM inference optimization on other emerging heterogeneous accelerator platforms as well.

The remainder of this paper is organized as follows: Section 2 introduces related work. Section 3 introduces Opt4GPTQ. Section 4 presents the experimental setup and results evaluation. Finally, Section 5 concludes the paper and discusses future research directions.

## II. RELATED WORK

Existing efficient LLM inference frameworks include LMDeploy [14], Text Generation Inference (TGI) [15], and vLLM. LMDeploy focuses on optimizing GPU performance through low-level operator tuning and scheduling strategies, aiming to achieve low inference latency and high throughput. It also integrates technologies such as FlashAttention to further enhance efficiency. Furthermore, LMDeploy is compatible with various hardware platforms and provides multimodal processing capabilities to meet the needs of enterprise-level real-time applications.

TGI aims to provide production-grade text generation services, focusing on stability and high throughput. TGI meets enterprise-level requirements such as multi-tenancy and security, and provides efficient inference on various hardware environments.

vLLM introduces the PagedAttention mechanism, which partitions the KV cache for each sequence into multiple discontinuous memory blocks. This approach reduces memory fragmentation and over-allocation, thereby improving memory utilization, especially in scenarios with long sequences and high concurrency. Furthermore, vLLM uses continuous batching to dynamically merge multiple requests into a single batch, thereby improving GPU utilization and throughput. However, existing frameworks, including vLLM, are primarily optimized for specific GPU architectures, leaving room for further optimization, particularly at the kernel level, in terms of adaptability to other heterogeneous accelerator platforms.

Quantization techniques aim to reduce computational and memory requirements by using low-precision weights and activation functions and leveraging specialized compute cores to accelerate inference. Representative quantization methods include AWQ [16] and GPTQ, which have been widely used for LLM inference. However, our research has found that applying these quantization methods to different heterogeneous computing platforms can sometimes lead to reduced efficiency due to hardware-specific bottlenecks. This observation highlights the need for platform-specific kernel-level optimizations to fully leverage the capabilities of heterogeneous accelerators and ensure effective deployment across diverse hardware environments.

## III. METHOD

This section introduces Opt4GPTQ, which integrates three strategies: Shared Memory Buffering Optimization (SMB-Opt), Vectorized Memory Loading Optimization (VML-Opt), and Inline Assembly-Level Optimization (ILA-Opt).

### A. SMB-Opt

Figure 1 illustrates the SMB-Opt method, which consists of two main phases: Phase 1 and Phase 2. Local memory is used to store the data that needs to be processed, and it is the private memory for each thread. Thread Block 0 and Thread Block 1 represent the thread blocks, Shared Memory refers to the shared memory section, and the bottom part represents global memory. “Wait” represents thread synchronization, ensuring that all threads have completed the shared memory operations before proceeding with the execution of subsequent code. In Phase 1, data flows from local memory to Thread Block 0 and Thread Block 1, where the threads within the block process the data and store partial intermediate results in shared memory. In Phase 2, the thread with index 0 in each Thread Block uses the `atomicAdd` operation to write the intermediate results stored in the shared memory back to the global memory, effectively reducing the number of global memory accesses.

This paper proposes a memory access optimization strategy using shared memory buffering for the `atomicAdd` opera-

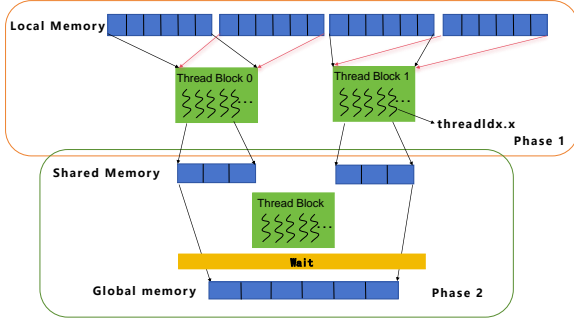


Fig. 1. Atomic operation optimization

tion, as shown in Algorithm 1: First, a piece of shared memory is allocated to each thread block to aggregate intermediate calculation results; second, each thread accumulates its own calculation results into this shared memory, as shown in Equations (1) and (2).

$$\text{block\_result}[0] = \sum_{m=0}^{M-1} (\text{result}01) \quad (1)$$

$$\text{block\_result}[1] = \sum_{m=0}^{M-1} (\text{result}23) \quad (2)$$

$\text{block\_result}[0]$  and  $\text{block\_result}[1]$  point to the requested shared memory.  $\text{result}01$  and  $\text{result}23$  are used to store the calculation results of each thread. The summary results are stored in  $\text{block\_result}[0]$  and  $\text{block\_result}[1]$ .

Finally, a single thread writes the aggregation result from the shared memory to the global memory through atomic operations. This optimization significantly reduces memory overhead by reducing the number of atomic operations and the frequency of global memory access, as shown in Equations (3)–(5).

$$\text{out} = \text{c\_item\_ptr}(\text{offset}_m, n) \quad (3)$$

$$\text{atomicAdd}(\text{out}, \text{block\_result}[0]) \quad (4)$$

$$\text{atomicAdd}(\text{out} + 1, \text{block\_result}[1]) \quad (5)$$

$\text{out}$  represents the starting address of the global memory location to be written.  $\text{atomicAdd}$  performs an atomic addition operation at the specified global memory location. Specifically, the addition of  $\text{block\_result}[0]$  and  $\text{block\_result}[1]$  is performed separately and added to the specified memory location.

## B. VML-Opt

By vectorizing memory access, two half-type elements are read from global memory each time instead of one half-type element, effectively reducing the number of global memory accesses.

## Algorithm 1 SMB-Opt

---

```

1: Input: Matrix  $\text{block}_c$  of size  $m \times n$ 
2: Output: Accumulated results in  $\text{block\_result}[0]$  and  $\text{block\_result}[1]$ 
3: Define shared memory array  $\text{block\_result}[2]$ 
4: if  $\text{threadIdx}.x == 0$  then
5:   Initialize  $\text{block\_result}[0]$  and  $\text{block\_result}[1]$  to  $\text{make\_half2}(0, 0)$ 
6: end if
7:  $\_\_\text{syncthreads}()$ 
8: for each row  $m$  in  $\text{block}_c$  do
9:   Convert values to half precision and pack into  $\text{half2}$ 
10:  Accumulate into  $\text{block\_result}$ 
11: end for
12:  $\_\_\text{syncthreads}()$ 
13: if  $\text{threadIdx}.x == 0$  then
14:  Write  $\text{block\_result}[0]$  and  $\text{block\_result}[1]$  to global memory using  $\text{atomicAdd}()$ 
15: end if

```

---

## Algorithm 2 VML-Opt

---

```

1: Input:
2: Matrix  $a_*$  of size  $M \times K$ 
3: Offset values  $\text{offset}_m, \text{offset}_k$ 
4: Thread index  $t$ 
5: Permutation array  $b\_q\_perm$  (optional)
6: Output: Loaded data stored in shared memory  $\text{block}_a[m\_count][\text{BLOCK\_KN\_SIZE}]$ 
7: if  $\text{offset}_k + t \leq \text{end}_k$  then
8:   for  $m = 0$  to  $m\_count - 1$  do
9:      $a\_ptr \leftarrow a\_item\_ptr(\text{offset}_m + m, 0)$ 
10:     $\text{block}_a\_ptr \leftarrow \text{block}_a[m]$ 
11:    if  $b\_q\_perm$  is not null then
12:       $a0\_h2 \leftarrow \text{half2}(a\_ptr[b\_q\_perm[\text{offset}_k + t]])$ 
13:    else
14:       $a0\_h2 \leftarrow \text{half2}(a\_ptr[\text{offset}_k + t])$ 
15:    end if
16:     $\text{block}_a\_ptr[t] \leftarrow \_\_\text{low2half}(a0\_h2)$ 
17:     $\text{block}_a\_ptr[t + 1] \leftarrow \_\_\text{high2half}(a0\_h2)$ 
18:   end for
19: end if

```

---

As shown in Algorithm 2, when loading the input matrix  $a$  from Equation (1) into shared memory, two half-type elements are combined into a single temporary variable, as shown in Equation (6).

$$a0\_h2 = \text{*reinterpret\_cast} < \text{half2*} > (\&a\_ptr[m]) \quad (6)$$

The  $\text{reinterpret\_cast}$  serves to re-interpret the address of  $a\_ptr[m]$  as a pair of half-types, which means it treats the originally contiguous two half-type data blocks as a combined structure containing two half-type elements. This structure, conceptually representing two half-type elements, allows access to both half-type elements simultaneously. This

---

**Algorithm 3** ILA-Opt

---

```
1: Input:  $a, b, c \in \mathbb{R}^2$  (half2)
2: Output:  $r_1, r_2 \in \mathbb{R}^2$  (half2)
3: Function hip_hfma2( $a, b, c$ )
4:   Declare  $r_1$ 
5:   Inline assembly: v_mad_f16 %0, %1, %2, %3
6:   Output:  $\%0 = r_1$ , Inputs:  $a, b, c$ 
7:   return  $r_1$ 
8: End Function
9: Function hip_hadd2( $a, b$ )
10:  Declare  $r_2$ 
11:  Inline assembly: v_add_f16 %0, %1, %2
12:  Output:  $\%0 = r_2$ , Inputs:  $a, b$ 
13:  return  $r_2$ 
14: End Function
```

---

operation dereferences the pointer, resulting in a structure containing two half-type elements, which is then assigned to  $a_0\_h2$ .

The assigned structure  $a_0\_h2$ , which contains two half-type elements, is then split into two separate half-type elements, as shown in Equations (7) and (8).

$$\text{block\_a\_ptr}(t) = \text{\_\_low2half}(a_0\_h2) \quad (7)$$

$$\text{block\_a\_ptr}(t+1) = \text{\_\_high2half}(a_0\_h2) \quad (8)$$

`\_\_low2half( $a_0\_h2$ )` extracts the first half-type element from  $a_0\_h2$  and stores it into the shared memory location  $\text{block\_a\_ptr}[t]$ . Similarly, `\_\_high2half( $a_0\_h2$ )` extracts the second half-type element from  $a_0\_h2$  and stores it into the shared memory location  $\text{block\_a\_ptr}[t+1]$ .

### C. ILA-Opt

ILA-Opt employs an instruction-level optimization strategy tailored to the hardware characteristics of the HYGON DCU. It replaces CUDA built-in functions `_hadd2` and `_hfma2` with custom inline assembly implementations based on the Graphics Core Next (GCN)/Vector Operations with 3 Operands (VOP3) instruction set. By directly invoking hardware-native vectorized half-precision addition (`v_add_f16`) and fused multiply-add (`v_mad_f16`) instructions, ILA-Opt reduces compiler abstraction overhead while achieving single-instruction multiple-operation (SIMO) execution. Additionally, inline assembly constraints enforce vector general-purpose register (VGPR) residency, effectively minimizing redundant data movement.

As shown in Algorithm 3, the rewritten `_hfma2` function `hip_hfma2` calls the `v_mad_f16` instruction and replaces the original CUDA function with an inline assembly implementation. This modification directly leverages the hardware-native `v_mad_f16`, and through the use of the GCN/VOP3 instruction set, enables SIMD execution. The execution method of this instruction is described in Equation (9).

$$r = a \times b + c \quad (9)$$

$a$ ,  $b$ , and  $c$  all store two half-type elements, so in fact, two half-type elements are multiplied and added.

As shown in Algorithm 3, the rewritten `hip_hadd2` function calls the `v_add_f16` instruction, which mainly performs the addition of two half-precision floating-point vectors, so that the addition operation can be performed directly at the hardware level. The execution method of this instruction is presented in Equation (10).

$$r = a + b \quad (10)$$

$a$ ,  $b$ , and  $r$  all store two half-type elements.

## IV. EXPERIMENTS

### A. Experimental environment

The experimental platform based on the HYGON DCU Z100 heterogeneous accelerator, and the ShareGPT\_V3\_unfiltered\_cleaned\_split dataset [17] is employed for throughput evaluation. The ARC [18] dataset is employed for accuracy evaluation. The ARC question set is partitioned into a Challenge Set (ARC\_C) and an Easy Set (ARC\_E). To enhance the robustness of the method, six models are used - Meta-Llama-3-8B-GPTQ [19], Llama-2-7B-GPTQ [20], CodeLlama-7B-GPTQ [21], LLaMa-13B-GPTQ, Qwen1.5-4B-Chat-GPTQ-Int4 [22] and Qwen1.5-1.8B-Chat-GPTQ-Int4, while the generation throughput, inference latency and inference accuracy of vLLM are used as the main performance indicators [23].

To ensure the reliability of the experimental results and minimize the impact of randomness and errors, the study repeated the experiment 15 times to enhance the scientific rigor of the findings. The final results were presented as the average of the 15 experimental trials.

### B. Baseline

This study establishes a performance evaluation baseline based on the non-optimized vLLM serving system [24]. The ShareGPT\_V3\_unfiltered\_cleaned\_split dataset is used for throughput evaluation, and the ARC dataset is used for accuracy evaluation. In this baseline setting, the input weights and activation values of the vLLM serving system are stored in FP16 format. Each evaluation run processes a single batch containing 32 prompts, and GPTQ 4-bit quantization is enabled to improve inference efficiency. Other configuration parameters use the default settings of vLLM. This baseline aims to provide a reference for subsequent model optimization and performance improvement, and we comprehensively evaluate the performance of the quantized model on the HYGON DCU Z100 heterogeneous accelerator.

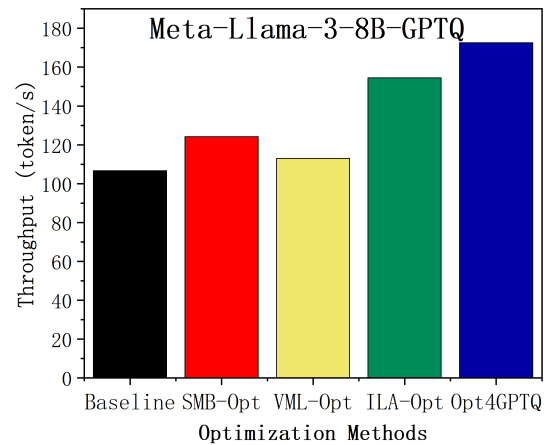
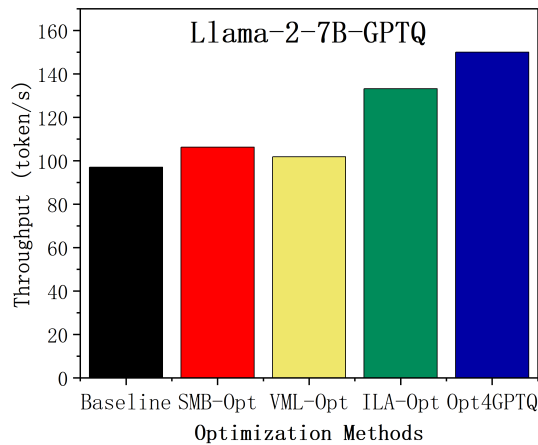
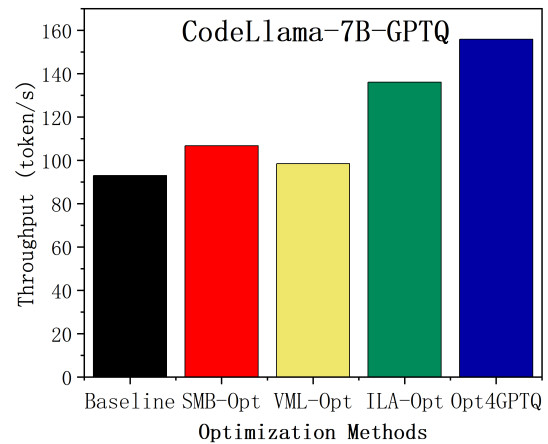
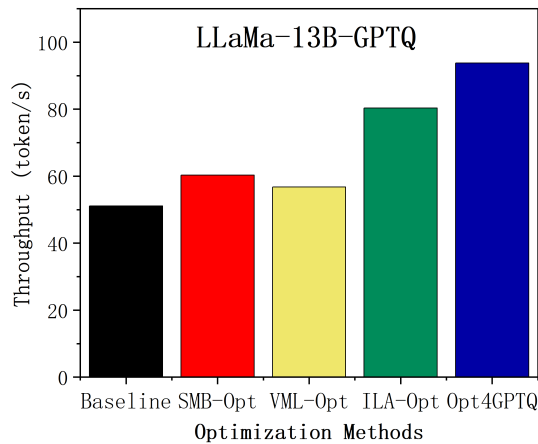
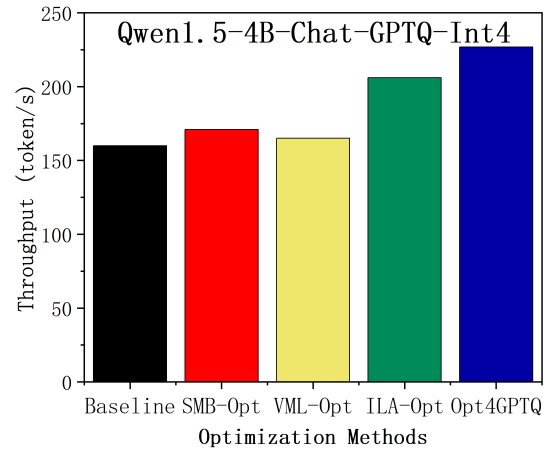
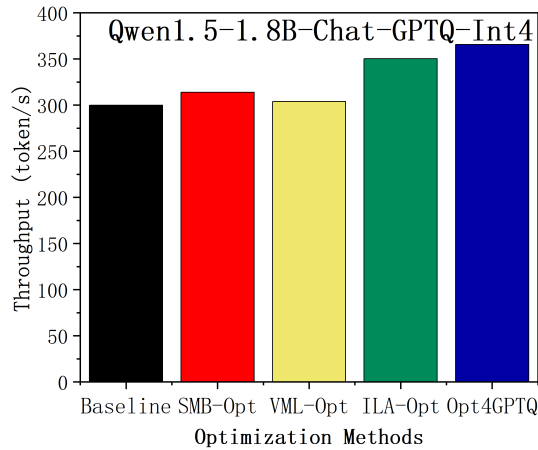


Fig. 2. Inference throughput comparison of vLLM across different models before and after applying SMB-Opt, VML-Opt, ILA-Opt, and Opt4GPTQ.

### C. Throughput Evaluation

The inference throughput improvements achieved by different models under the same optimization methods vary due

to differences in model size, architecture, and computational characteristics. Larger models, such as LLaMa-13B-GPTQ and Meta-Llama-3-8B-GPTQ, exhibit more significant gains

from shared memory and instruction-level optimizations because of their higher parameter counts and memory access demands. In contrast, smaller models, such as Qwen1.5-1.8B-Chat-GPTQ-Int4, experience limited benefits as they are less constrained by memory and compute resources. Additionally, factors such as the number of Transformer layers, operator density, quantization characteristics, input sequence lengths, and concurrency levels further influence the effectiveness of these optimizations.

The experimental results presented in this section follow the model order: Qwen1.5-4B-Chat-GPTQ-Int4, Qwen1.5-1.8B-Chat-GPTQ-Int4, LLaMa-13B-GPTQ, CodeLlama-7B-GPTQ, Llama-2-7B-GPTQ, and Meta-Llama-3-8B-GPTQ, as shown in Figure 2.

1) *Throughput Evaluation of SMB-Opt*: As shown in Figure 2, after applying the SMB-Opt optimization method, vLLM achieved inference throughput improvements of 6.83%, 4.94%, 17.98%, 14.74%, 9.50%, and 16.43% for the six models: Qwen1.5-4B-Chat-GPTQ-Int4, Qwen1.5-1.8B-Chat-GPTQ-Int4, LLaMa-13B-GPTQ, CodeLlama-7B-GPTQ, Llama-2-7B-GPTQ, and Meta-Llama-3-8B-GPTQ, respectively. The optimization mainly reduces global memory access overhead by leveraging shared memory buffers, which is particularly effective on larger models such as LLaMa-13B-GPTQ and Meta-Llama-3-8B-GPTQ, where throughput gains reached 17.98% and 16.43%.

2) *Throughput Evaluation of VML-Opt*: After applying the VML-Opt optimization method, vLLM achieved throughput improvements of 3.11%, 1.36%, 11.03%, 5.88%, 4.91%, and 5.89% across the same six models. Compared to SMB-Opt, VML-Opt offers more moderate gains, with the most notable improvement of 11.03% observed on LLaMa-13B-GPTQ. This is attributed to enhanced vectorized memory loading efficiency, which mitigates data transfer bottlenecks in the quantization process.

3) *Throughput Evaluation of ILA-Opt*: The ILA-Opt optimization method delivered significant throughput improvements of 28.74%, 16.75%, 57.19%, 46.30%, 37.26%, and 44.81% across the same six models. The method achieves these gains by directly utilizing hardware-native vectorized half-precision instructions through inline assembly, leading to efficient execution at the instruction level. ILA-Opt proved particularly effective on LLaMa-13B-GPTQ and CodeLlama-7B-GPTQ, with throughput improvements exceeding 57.19% and 46.30%, respectively.

4) *Throughput Evaluation of Opt4GPTQ*: By integrating SMB-Opt, VML-Opt, and ILA-Opt, the Opt4GPTQ method achieved cumulative throughput improvements of 41.77%, 21.93%, 84.42%, 67.55%, 54.55%, and 61.78% for the same six models. Opt4GPTQ demonstrated the highest overall gains, especially on LLaMa-13B-GPTQ and CodeLlama-7B-GPTQ, where throughput was improved by 84.42% and 67.55%. The cumulative optimization effects indicate that combining memory access reduction, vectorized loading, and instruction-level acceleration is effective for fully exploiting the hardware potential of platforms in GPTQ inference scenarios.

#### D. Latency Evaluation

The experimental results presented in this section follow the model order: Qwen1.5-4B-Chat-GPTQ-Int4, Qwen1.5-1.8B-Chat-GPTQ-Int4, LLaMa-13B-GPTQ, CodeLlama-7B-GPTQ, Llama-2-7B-GPTQ, and Meta-Llama-3-8B-GPTQ, as shown in Figure 3.

1) *Latency Evaluation of SMB-Opt*: As shown in Figure 3, the SMB-Opt optimization method effectively reduced inference latency by improving global memory access efficiency. Specifically, vLLM achieved latency reductions of 5.21%, 4.62%, 12.41%, 11.86%, 11.39%, and 7.48% across the six models: Qwen1.5-4B-Chat-GPTQ-Int4, Qwen1.5-1.8B-Chat-GPTQ-Int4, LLaMa-13B-GPTQ, CodeLlama-7B-GPTQ, Llama-2-7B-GPTQ, and Meta-Llama-3-8B-GPTQ, respectively. These results demonstrate that SMB-Opt brings moderate latency improvements, particularly for larger models with higher memory access overheads.

2) *Latency Evaluation of VML-Opt*: VML-Opt focused on enhancing memory load efficiency through vectorized memory operations. The latency reductions achieved by VML-Opt were relatively smaller compared to other methods, with improvements of 1.93%, 2.67%, 1.21%, 2.33%, 2.39%, and 0.55% for the six models in order. While VML-Opt offered limited latency gains, it contributed to overall efficiency by reducing data transfer overheads, especially in models with smaller computational bottlenecks.

3) *Latency Evaluation of ILA-Opt*: ILA-Opt provided significant latency reductions by leveraging hardware-native vectorized instructions. The achieved improvements were 30.91%, 19.42%, 36.97%, 36.98%, 37.0%, and 31.18% for Qwen1.5-4B-Chat-GPTQ-Int4 through Meta-Llama-3-8B-GPTQ, respectively. These results highlight that low-level instruction-level optimization can substantially accelerate inference, particularly for models where fused multiply-add operations dominate computation.

4) *Latency Evaluation of Opt4GPTQ*: The integrated Opt4GPTQ method, which combines SMB-Opt, VML-Opt, and ILA-Opt, achieved the most substantial latency reductions, with improvements of 47.96%, 25.18%, 51.35%, 49.73%, 49.81%, and 41.23% across the six models. The cumulative effect of memory access optimization, vectorized data loading, and hardware-level instruction tuning led to significant latency improvements, especially for larger models like LLaMa-13B-GPTQ and CodeLlama-7B-GPTQ.

#### E. Accuracy Evaluation

As shown in Tables I and II, we evaluated the inference accuracy of six model-Qwen1.5-4B-Chat-GPTQ-Int4, Qwen1.5-1.8B-Chat-GPTQ-Int4, LLaMa-13B-GPTQ, CodeLlama-7B-GPTQ, Llama-2-7B-GPTQ, and Meta-Llama-3-8B-GPTQ on the ARC\_C and ARC\_E datasets. Across all models and optimization methods (SMB-Opt, VML-Opt, ILA-Opt, Opt4GPTQ), the accuracy variations remained within 1 percentage point, with no consistent upward or downward trends. On ARC\_C, most models exhibited fluctuations within 0.68 percentage points, while on ARC\_E, the largest variation

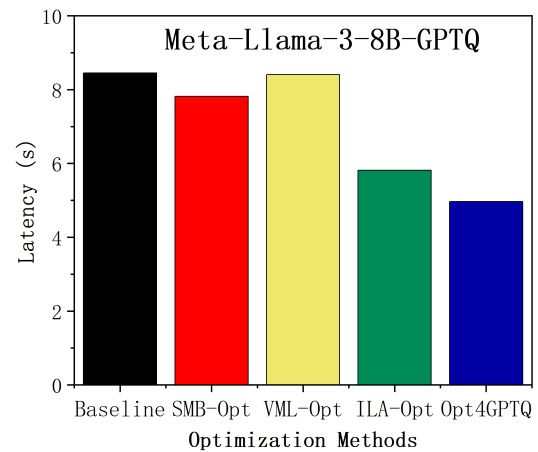
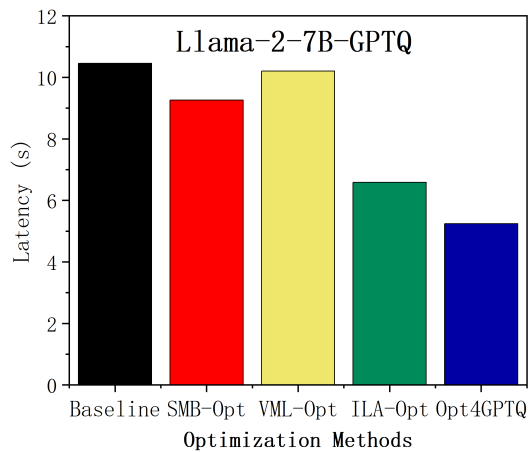
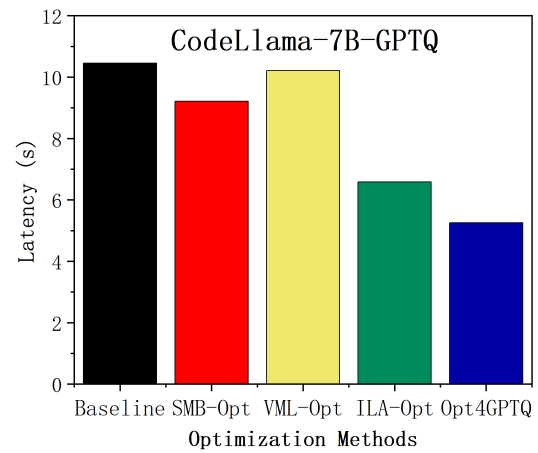
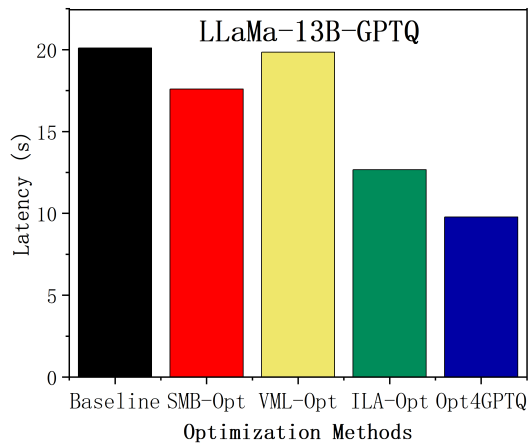
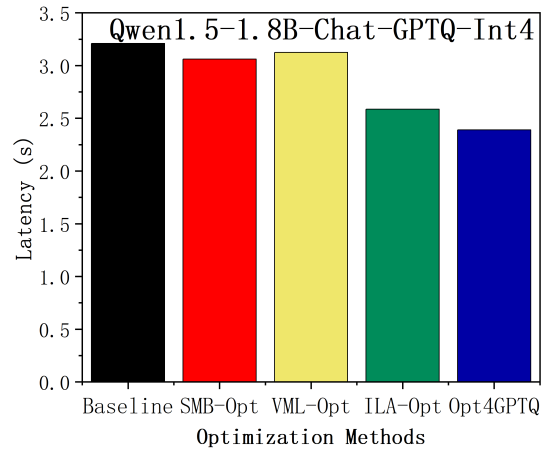
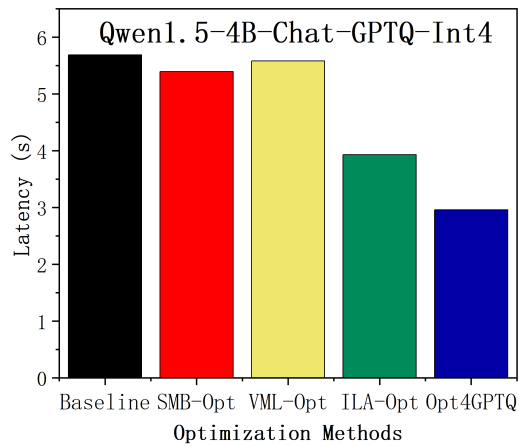


Fig. 3. Inference latency comparison of vLLM across different models before and after applying SMB-Opt, VML-Opt, ILA-Opt, and Opt4GPTQ.

was 0.89 percentage points for LLaMa-13B-GPTQ. Notably, Qwen1.5-4B-Chat-GPTQ-Int4 showed no measurable change. These results indicate that the proposed optimization methods

have a negligible impact on inference accuracy, maintaining the original precision with excellent stability.

TABLE I

INFERENCE ACCURACY OF vLLM ON DIFFERENT MODELS USING THE ARC\_C DATASET BEFORE AND AFTER APPLYING SMB-OPT, VML-OPT, ILA-OPT, AND OPT4GPTQ.

Models	Baseline	SMB-Opt	VML-Opt	ILA-Opt	Opt4GPTQ
Meta-Llama-3-8B-GPTQ	75.25%	74.92%	74.92%	74.92%	75.25%
Llama-2-7B-GPTQ	35.59%	36.27%	35.25%	35.25%	35.59%
CodeLlama-7B-GPTQ	27.81%	28.47%	28.47%	28.47%	29.15%
LLaMa-13B-GPTQ	39.32%	39.66%	39.66%	40.00%	39.32%
Qwen1.5-1.8B-Chat-GPTQ-Int4	48.81%	48.81%	48.81%	48.79%	48.81%
Qwen1.5-4B-Chat-GPTQ-Int4	56.27%	55.59%	56.27%	56.27%	55.59%

TABLE II

INFERENCE ACCURACY OF vLLM ON DIFFERENT MODELS USING THE ARC\_R DATASET BEFORE AND AFTER APPLYING SMB-OPT, VML-OPT, ILA-OPT, AND OPT4GPTQ.

Models	Baseline	SMB-Opt	VML-Opt	ILA-Opt	Opt4GPTQ
Meta-Llama-3-8B-GPTQ	87.30%	87.48%	87.30%	87.30%	87.30%
Llama-2-7B-GPTQ	47.80%	47.97%	48.59%	48.15%	47.44%
CodeLlama-7B-GPTQ	27.51%	27.87%	27.87%	27.87%	27.87%
LLaMa-13B-GPTQ	50.79%	51.68%	51.68%	51.50%	50.79%
Qwen1.5-1.8B-Chat-GPTQ-Int4	69.49%	69.14%	69.49%	69.14%	69.14%
Qwen1.5-4B-Chat-GPTQ-Int4	70.19%	70.19%	70.19%	70.19%	70.19%

## V. CONCLUSION

This study proposes Opt4GPTQ, a platform-level optimization strategy designed to enhance the inference efficiency of vLLM on heterogeneous AI acceleration platforms, thereby addressing the deployment challenges posed by emerging hardware architectures. Opt4GPTQ targets the GPTQ 4-bit quantized GEMM kernel within the vLLM serving system and integrates three key techniques: Shared Memory Buffering (SMB-Opt), Vectorized Memory Loading (VML-Opt), and Inline-Level Assembly Optimization (ILA-Opt). Experimental evaluations demonstrate that Opt4GPTQ achieves inference efficiency enhancement, improving throughput and reducing latency across various LLMs, while maintaining accuracy. This work provides practical deployment experience and highlights the necessity of platform-specific engineering optimizations for realizing efficient LLM inference on heterogeneous AI accelerators. For future work, we plan to extend our study by analyzing how the speedup varies with different batch sizes and by evaluating performance when parallel decoding is enabled. Moreover, we will validate the applicability of our method on different heterogeneous computing platforms to further demonstrate its generalization capability.

## ACKNOWLEDGMENT

This work was supported in part by the National Natural Science Foundation of China (NSFC) under Grants 62072287 and W2412090, in part by the HYGON Industry Ecological Cooperation Organization (HIECO) under Grant 202407027775, and in part by the Shandong Provincial Natural Science Foundation under Grant ZR2024ME230.

## REFERENCES

[1] H. Touvron, T. Lavril, G. Izacard, X. Martinet, M.-A. Lachaux, T. Lacroix, B. Rozière, N. Goyal, E. Hambro, F. Azhar, et al., "Llama: Open and efficient foundation language models," arXiv Preprint arXiv:2302.13971, 2023.

[2] C. Leiter, R. Zhang, Y. Chen, J. Belouadi, D. Larionov, V. Fresen, and S. Eger, "Chatgpt: A meta-analysis after 2.5 months," *Machine Learning with Applications*, vol. 16, p. 100541, 2024.

[3] A. Liu, B. Feng, B. Wang, B. Liu, C. Zhao, C. Deng, C. Ruan, D. Dai, D. Guo, et al., "Deepseek-v2: A strong, economical, and efficient mixture-of-experts language model," arXiv Preprint arXiv:2405.04434, 2024.

[4] Gemini Team, R. Anil, S. Borgeaud, J.-B. Alayrac, J. Yu, R. Soricut, J. Schalkwyk, A. M. Dai, A. Hauth, K. Millican, et al., "Gemini: a family of highly capable multimodal models," arXiv Preprint arXiv:2312.11805, 2023.

[5] Z. Zhou, X. Ning, K. Hong, T. Fu, J. Xu, S. Li, Y. Lou, L. Wang, Z. Yuan, X. Li, et al., "A survey on efficient inference for large language models," arXiv Preprint arXiv:2404.14294, 2024.

[6] J. Zhou, Y. Cao, Q. Lu, W. Zhang, X. Liu, and W. Ni, "Industrial Large Model: Toward A Generative AI for Industry," in 2024 IEEE Canadian Conf. Elect. Comput. Eng. (CCECE), 2024, pp. 80–81.

[7] W. Kwon, Z. Li, S. Zhuang, Y. Sheng, L. Zheng, C. H. Yu, J. Gonzalez, H. Zhang, and I. Stoica, "Efficient memory management for large language model serving with pagedattention," in Proc. 29th Symp. Oper. Syst. Princ., 2023, pp. 611–626.

[8] X. Zhu, J. Li, Y. Liu, C. Ma, and W. Wang, "A survey on model compression for large language models," *Trans. Assoc. Comput. Linguistics*, vol. 12, pp. 1556–1577, 2024.

[9] J. Lang, Z. Guo, and S. Huang, "A comprehensive study on quantization techniques for large language models," in 2024 4th Int. Conf. Artif. Intell. Robot. Commun. (ICAIRC), 2024, pp. 224–231.

[10] E. Frantar, S. Ashkboos, T. Hoefler, and D. Alistarh, "Gptq: Accurate post-training quantization for generative pre-trained transformers," arXiv Preprint arXiv:2210.17323, 2022.

[11] G. Wilkins, S. Keshav, and R. Mortier, "Offline energy-optimal llm serving: Workload-based energy models for llm inference on heterogeneous systems," *ACM SIGENERGY Energy Informatics Rev.*, vol. 4, no. 5, pp. 113–119, 2024.

[12] T. Yang, P. Feng, Q. Guo, J. Zhang, J. Ning, X. Wang, and Z. Mao, "AutoHMA-LLM: Efficient task coordination and execution in heterogeneous multi-agent systems using hybrid large language models," *IEEE Trans. Cogn. Commun. Netw.*, 2025 (in press).

[13] J. Jia, X. Lin, F. Lin, and Y. Liu, "DCU-CHK: Checkpointing for large-scale CPU-DCU heterogeneous computing systems," *CCF Trans. High Perform. Comput.*, vol. 6, no. 5, pp. 519–532, 2024.

[14] InternLM Team, "LMDeploy: A toolkit for deploying LLM models," GitHub Repository, 2025. [Online]. Available: <https://github.com/InternLM/lmdeploy>

[15] Hugging Face, "Text Generation Inference," 2022. [Online]. Available: <https://github.com/huggingface/text-generation-inference>

[16] J. Lin, J. Tang, H. Tang, S. Yang, W.-M. Chen, W.-C. Wang, G. Xiao, X. Dang, C. Gan, and S. Han, "Awq: Activation-aware weight quantization for on-device llm compression and acceleration," *Proc. Mach. Learn. Syst.*, vol. 6, pp. 87–100, 2024.

[17] Gliang1001, "ShareGPT\_V3\_unfiltered\_cleaned\_split," ModelScope Dataset, 2023. [Online]. Available: [https://www.modelscope.cn/datasets/gliang1001/ShareGPT\\_V3\\_unfiltered\\_cleaned\\_split](https://www.modelscope.cn/datasets/gliang1001/ShareGPT_V3_unfiltered_cleaned_split)

[18] P. Clark, I. Cowhey, O. Etzioni, T. Khot, A. Sabharwal, C. Schoenick, and O. Tafjord, "Think you have solved question answering? try arc, the ai2 reasoning challenge," arXiv Preprint arXiv:1803.05457, 2018.

[19] A. Grattafiori, A. Dubey, A. Jauhri, A. Pandey, A. Kadian, A. Al-Dahle, A. Letman, A. Mathur, A. Schelten, A. Vaughan, et al., "The llama 3 herd of models," arXiv Preprint arXiv:2407.21783, 2024.

[20] H. Touvron, L. Martin, K. Stone, P. Albert, A. Almahairi, Y. Babaei, N. Bashlykov, S. Batra, P. Bhargava, S. Bhosale, et al., "Llama 2: Open foundation and fine-tuned chat models," arXiv Preprint arXiv:2307.09288, 2023.

[21] B. Rozière, J. Gehring, F. Gloeckle, S. Sootla, I. Gat, X. E. Tan, Y. Adi, J. Liu, R. Sauvestre, T. Remez, et al., "Code llama: Open foundation models for code," arXiv Preprint arXiv:2308.12950, 2023.

[22] J. Bai, S. Bai, Y. Chu, Z. Cui, K. Dang, X. Deng, Y. Fan, W. Ge, Y. Han, F. Huang, et al., "Qwen technical report," arXiv Preprint arXiv:2309.16609, 2023.

[23] Y. Chang, X. Wang, J. Wang, Y. Wu, L. Yang, K. Zhu, H. Chen, X. Yi, C. Wang, Y. Wang, et al., "A survey on evaluation of large language models," *ACM Trans. Intell. Syst. Technol.*, vol. 15, no. 3, pp. 1–45, 2024.

[24] OpenDAS, “vllm-v0.3.3-dtk24.04,” 2024. [Online]. Available: <https://developer.sourcefind.cn/codes/OpenDAS/vllm/-/tree/vllm-v0.3.3-dtk24.04>